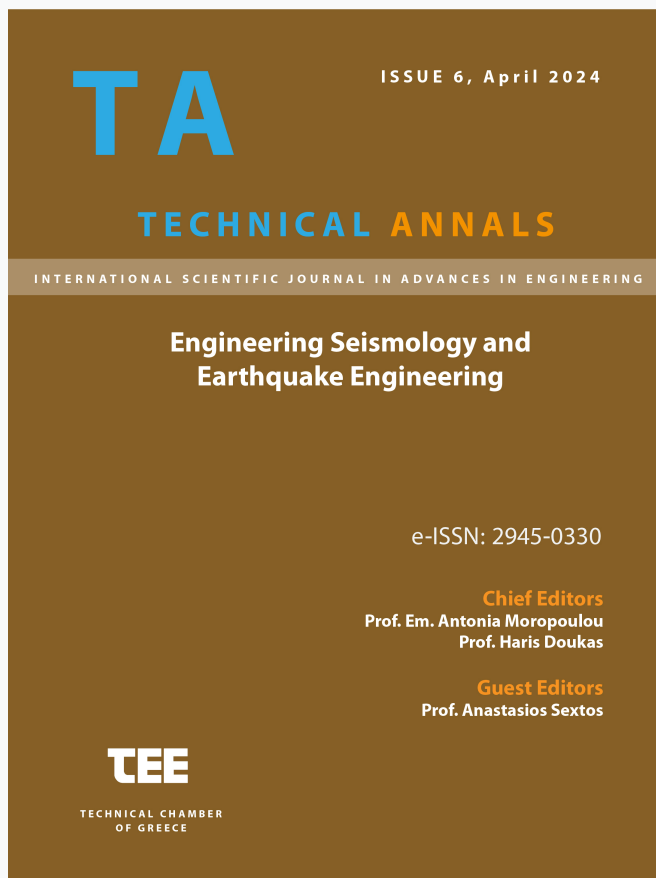


## Technical Annals

Vol 1, No 6 (2024)

Technical Annals



### Novel Method for the Stochastic Generation of Hazard-Consistent Artificial Accelerograms: A practical application

Hera Yanni, Michalis Fragiadakis, Ioannis P. Mitseas

doi: [10.12681/ta.36879](https://doi.org/10.12681/ta.36879)

Copyright © 2024, Hera Yanni, Michalis Fragiadakis, Ioannis Mitseas



This work is licensed under a [Creative Commons Attribution-NonCommercial-ShareAlike 4.0](https://creativecommons.org/licenses/by-nc-sa/4.0/).

### To cite this article:

Yanni, H., Fragiadakis, M., & Mitseas, I. P. (2024). Novel Method for the Stochastic Generation of Hazard-Consistent Artificial Accelerograms: A practical application. *Technical Annals*, 1(6). <https://doi.org/10.12681/ta.36879>

# Novel Method for the Stochastic Generation of Hazard-Consistent Artificial Accelerograms: A practical application

Hera Yanni<sup>1</sup>[0009-0003-0314-0519], Michalis Fragiadakis<sup>1</sup>[0000-0002-0698-822X] and  
Ioannis P. Mitseas<sup>1,2</sup>[0000-0001-5219-1804]

<sup>1</sup>National Technical University of Athens, 9 Iroon Polytechniou St., 15780 Athens, Greece

<sup>2</sup>School of Civil Engineering, University of Leeds, Leeds, UK  
heragian@mail.ntua.gr, mfrag@mail.ntua.gr,  
Imitseas@mail.ntua.gr, I.Mitseas@leeds.ac.uk

**Abstract.** In contemporary engineering practice, the investigation of the dynamic response of structures through time-history analysis requires the use of suites of acceleration ground motions. The paper studies the response of structures subjected to a novel methodology for the generation of target spectrum compatible artificial accelerograms. Existing spectrum-based models are used for the ground motion generation, whereas hazard consistency is achieved by matching these records either to a design spectrum or to a ground motion model. The obtained suites are used for the non-linear response history analysis (NRHA) of a benchmark multi-degree-of-freedom structure. Two study examples are presented. In the first example the generated suite matches only a spectral mean and in the second example the suite matches both the target spectral mean and variability. The results indicate that using the generated ground motion suites for the target NRHAs produces results that are consistent with record selection algorithms, thus confirming the efficiency of the proposed methodology.

**Keywords:** artificial accelerogram, non-linear dynamic analysis, non-stationary, spectrum-compatible, variability, ground motion model.

## 1 Introduction

The increasing availability of powerful personal computers and advanced engineering software has facilitated the use of dynamic time-history analysis in everyday engineering practice. This type of analysis is deemed the most realistic for assessing the seismic behavior of structures, especially when non-linear response is expected. Non-linear response history analysis (NRHA) is influenced by multiple sources of uncertainties stemming from the calibration of the non-linear structural model (e.g. material properties, design assumptions), as well as the modeling of the seismic excitation. The latter is recognized to have a significant effect on the seismic response of structures.

Accelerograms that model the input seismic motion for the NRHAs can be either previously recorded, synthetic or artificially generated. The most common practice followed

is the careful selection and scaling of recorded ground motion records from online databases; however, this approach still has limitations. Selected accelerograms are often recorded in other locations than the site of interest and correspond to different magnitude-distance scenarios and soil characteristics. Moreover, the scarcity of recorded ground motions of earthquakes with large magnitudes at small epicentral distances can often confine the analysis, especially for high-limit states like collapse. As a result, the task of selecting and scaling earthquake records remains a highly controversial issue in the literature [1], and various algorithms have been proposed [2–3] for addressing these challenges.

The use of artificially generated acceleration time-histories provides a valid alternative to circumvent the issues linked with the selection of recorded ground motions and is also recommended by seismic codes [4]. Their main advantage is that they can be modeled to have the desired target features that are required within the framework of dynamic analysis. The use of artificial accelerograms in seismic simulations has found widespread applications in the field of structural engineering, ranging from Monte Carlo Simulation techniques [5], to stochastic dynamics simulations [6–7] for structural reliability assessment. Furthermore, practice-oriented probabilistic models that model the seismic demand based on specific values assumed by an intensity measure can also use artificial ground motions [8].

Seismic codes do not propose specific methods for the generation of artificial accelerograms; they only define some basic requirements related to their matching to the design code spectrum. For example, Eurocode 8 [4] mainly requires that the mean response spectrum of the generated accelerograms should match the code's elastic response spectrum for 5% viscous damping. Therefore, engineers are focused on the target spectrum matching requirement and thus can choose from a wide range of proposed methods in the literature.

Given the inherently stochastic nature of earthquakes, artificial ground motion time-histories are typically generated as stochastic processes. The spectral representation method proposed by Shinozuka and Deodatis [9], is the most widespread method in the literature. The method simulates ground motion time-histories as a superposition of harmonic components with random phase angles. In this approach, the power spectral density (PSD) function is directly related to the amplitude of each harmonic, thus providing the basis for generating target spectrum-compatible accelerograms. As highlighted by Vanmarcke and Gasparini [10], spectrum compatibility can be achieved by matching the values of the PSD function of the ground motion to the response spectral values for a given damping ratio.

The desired ground motion time-histories for NRHAs that are simulated using the PSD function are typically non-stationary both in amplitude and frequency. Several methods have been proposed in order to generate fully non-stationary accelerograms. One approach is the use of an evolutionary power spectral density (EPSD) function, i.e. a PSD function that varies in time [11]. This is typically achieved by introducing an envelope function that modifies a stationary accelerogram both in time and in frequency in order to simulate the characteristic behavior of natural accelerograms [12,13]. Other approaches include using a real record as a seed [14,15]. For example, the method proposed by Cacciola [15] produces fully non-stationary accelerograms as the superposition of two waveforms: a

fully non-stationary counterpart modeled by a real accelerogram and a stationary process that is used to achieve spectrum compatibility.

Seismic response assessment through the NRHA requires the use of suites of hazard-consistent acceleration time-histories. Depending on the performance assessment type, hazard consistency may be achieved by matching the records either to a uniform hazard spectrum (UHS) which is typically a code spectrum [4], to a conditional mean spectrum (CMS) [16], or to a spectrum obtained from a ground motion model (GMM) [18]. NIST [18] mentions three types of performance assessment: intensity-based, scenario-based, and risk-based. More specifically, intensity-based assessment focuses on the seismic response of a structure for a specified ground motion intensity, which is typically defined as a 5% damped elastic spectral acceleration spectrum (e.g. a code spectrum). Scenario-based assessments compute the structural responses to user-specified seismic events that are defined by the earthquake magnitude and the distance of the source from the site of interest. The typical products of a scenario-based assessment are the average response of a structural parameter and the corresponding variability. Finally, risk-based assessments provide information on the response of a structure over a user-specified time period, involving multiple intensity-based assessments for the ground motion levels of interest.

Based on the objectives of the seismic performance assessment, there are cases where the input ground motions may match only a target mean response spectrum, while in other cases the variability of the response spectra should also be incorporated [18]. For example, in order to predict stable mean responses of structural parameters for a given intensity of shaking, matching ground motions to a target spectrum may be a suitable approach that enhances the confidence in the predictions of the mean structural responses for a given number of input ground motions. However, in applications where the prediction of both the mean value and variability of a structural parameter is required (e.g. estimation of collapse probabilities), the ground motions should be matched to a target spectral mean and the respective spectral variability.

Jayaram et al. [2] in their paper proposed a new algorithm for selecting ground motions that match a target response spectrum mean and variance. Moreover, they applied their proposed methodology to conduct NRHAs on single-degree-of-freedom (SDOF) and multi-degree-of-freedom (MDOF) systems in order to assess the influence of the consideration of the response spectrum variance on the structural response. They concluded that using ground motion suites that also match the target response spectrum variance increases the dispersion of the obtained structural responses. This dispersion, as observed in their analyses, impacts the distribution of structural responses, damage states, loss estimations, and the probability of structural collapse.

The paper studies the application of suites of fully non-stationary artificial accelerograms that have a target spectral mean and variability in order to achieve hazard consistency [12,19–21] on structural performance assessment. The model that is used first produces an ensemble of target spectra with a given mean and variability and then a methodology based on spectral representation method is used to generate the corresponding fully non-stationary ground motions. The stochastic methodology is briefly presented first, and it is followed by a numerical application where the NRHA of a benchmark multi-degree-of-freedom (MDOF) structure is carried out. The seismic hazard is quantified with

a GMM, and the impact of the spectrum variability matching on the structural response is assessed.

## 2 Generation of Artificial Accelerograms

A practical and computationally efficient methodology for the stochastic generation of suites of fully non-stationary artificial accelerograms that are compatible with a target spectral mean and a target variability [12,19–21] is employed. The artificial ground motion time histories are simulated as stochastic processes using existing spectrum-based models [15]. The seismic hazard is defined by a target spectrum or a GMM. Therefore, given the seismic scenario ( $M, R$ ) and the soil conditions, the target spectral mean and variability for each period are obtained. Based on those data, multiple target response spectra are generated as a random vector that follows the normal distribution. Artificial accelerograms whose response spectra individually match the produced spectra are subsequently generated. The basis for generating spectrum-compatible accelerograms relies on the relationship between the values of the power spectral density (PSD) function of the ground motion and the response spectral values for a given damping ratio [10,21]. Corrective iterations in the frequency domain are performed in order to achieve enhanced matching for controlling the variability. The methodology provides with suites of fully nonstationary artificial ground motion time histories that are compatible with a target spectral mean and a target variability, which then can be used to conduct NRHAs in structures.

### 2.1 Target spectra generation

The proposed methodology first produces a suite of target spectra  $S_a^{*j}(T_i, \zeta)$  that have a target spectral mean  $S_a^*(T_i, \zeta)$  and variability  $\beta^*(T_i, \zeta)$ , where  $\zeta$  is the target spectrum's damping ratio. In the case where a GMM is used for the analysis, the method relies on the empirically verified observation that the logarithmic spectral accelerations follow the normal distribution, characterized by a mean value and standard deviation [12,20]. Therefore, the target logarithmic spectral accelerations  $\ln[S_a^{*j}(T_i, \zeta)]$  at each period  $T_i$  can be modeled as a normally distributed (Gaussian) random variable with mean  $\ln[S_a^*(T_i, \zeta)]$  and standard deviation  $\sigma_{\ln(S_a)}^*(T_i, \zeta)$ :

$$\ln[S_a^{*j}(T_i, \zeta)] = \ln[S_a^*(T_i, \zeta)] + a_j \sigma_{\ln(S_a)}^*(T_i, \zeta) \quad (1)$$

where  $1 \leq j \leq n$ ,  $n$  is the total number of the generated accelerograms in a suite,  $a_j$  is a standard Gaussian random variable with mean value  $\mu_\alpha = 0$  and standard deviation  $\sigma_\alpha = 1$ , and  $T_i$  are period values of the response spectrum. The target mean in Eq. 1 is obtained from the GMM at the desired period range. The variability around the target spectrum is defined as the standard deviation of the natural logarithms of the spectral values given from the GMM, thus  $\beta^*(T_i, \zeta) = \sigma_{\ln(S_a)}^*(T_i, \zeta)$ . It is noted that Eq. 1 considers that the correlation  $\rho(T_i, T_j)$  between the spectral accelerations at different periods is equal to 1, thus assuming a perfect direct correlation. Based on Eq. 1, for a suite containing  $n$  accelerograms, each individual target response spectrum  $S_a^{*j}(T_i, \zeta)$ , can be produced as:

$$S_a^{*j}(T_i, \zeta) = S_a^*(T_i, \zeta) \exp [a_j \beta^*(T_i, \zeta)] \quad (2)$$

In the case of a smooth code spectrum [26], each of the suite's accelerograms is generated compatible with a specific target response spectrum  $S_a^{*j}(T_i, \zeta)$  that is defined as:

$$S_a^{*j}(T_i, \zeta) = S_a^*(T_i, \zeta) + a_j \sigma_{S_a^*}^*(T_i, \zeta) \quad (3)$$

In this case, the variability around the target spectrum is defined as the coefficient of variation (CoV) for each period:

$$\beta^*(T_i, \zeta) = CoV = \frac{\sigma_{S_a^*}^*(T_i, \zeta)}{S_a^*(T_i, \zeta)} \quad (4)$$

Next,  $\sigma_{S_a^*}^*(T_i, \zeta)$  is calculated as  $\sigma_{S_a^*}^*(T_i, \zeta) = \beta^*(T_i, \zeta) S_a^*(T_i, \zeta)$ , and Eq. (3) becomes:

$$S_a^{*j}(T_i, \zeta) = S_a^*(T_i, \zeta) [1 + a_j \beta^*(T_i, \zeta)] > 0 \quad (5)$$

In order to ensure that the target spectrum  $S_a^{*j}(T_i, \zeta)$  will take no negative values, the value of  $[1 + a_j \beta^*(T_i, \zeta)]$  must be greater than zero. This results in the following limit for the values of  $a_j$ :

$$a_j > - \frac{1}{\beta^*(T_i, \zeta)} \quad (6)$$

## 2.2 Generation of the Artificial Accelerograms

The target spectrum compatible artificial accelerograms can be modeled using existing real earthquake ground motions as seed records. In this study, the Cacciola 2010 [15] method was employed, which generates fully non-stationary, spectrum compatible accelerograms by superimposing a seed record  $a_R(t)$  and a corrective term which is a quasi-stationary zero-mean Gaussian stochastic process, defined with the spectral representation method [16]:

$$a_g(t) = a_{sc} a_R(t) + \varphi(t) \sum_{i=1}^N A_i(\omega) \cos(\omega_i t + \theta_i) \quad (7)$$

In the first part of Eq. 7  $a_R(t)$  is a recorded accelerogram used as a seed and  $a_{sc}$  is a scaling coefficient associating the target spectral acceleration  $S_a^*(\omega_i, \zeta)$  with the recorded accelerogram's spectral acceleration  $S_a^R(\omega_i, \zeta)$ :

$$a_{sc} = \min \left[ \frac{S_a^*(\omega_i, \zeta)}{S_a^R(\omega_i, \zeta)} \right] \quad (8)$$

Moreover, if  $a_{sc} > 1$ , then  $a_{sc} = 1$  is assumed instead [15]. In the second part of Eq. 7,  $\varphi(t)$  is the time-modulating function,  $N$  is the number of harmonics to be superimposed,  $\omega_i$  is the angular frequency of the  $i^{\text{th}}$  harmonic,  $\theta_i$  are random phase angles uniformly distributed over the interval  $[0, 2\pi]$ , and  $A_i(\omega)$  are the amplitudes, related to the one-sided PSD function of the stochastic process  $G(\omega_i)$  at each frequency  $\omega_i$  as:

$$A_i(\omega) = \sqrt{2G(\omega_i)\Delta\omega} \quad (9)$$

where  $\Delta\omega$  is the constant integration step. Spectrum compatibility is achieved by the computation of the one-sided PSD function  $G(\omega_i)$  [15]:

$$G(\omega_i) = \begin{cases} \frac{4\zeta}{\omega_i\pi - 4\zeta\omega_{i-1}} U \left[ \frac{S_a^{*2}(\omega_i, \zeta) - (a_{sc} S_a^R(\omega_i, \zeta))^2}{\eta_{X_i}^2(\omega_i, \zeta)} - \Delta\omega \sum_{k=1}^{i-1} G(\omega_k) \right] \times \\ \times \left[ \frac{S_a^2(\omega_i, \zeta) - (a_{sc} S_a^R(\omega_i, \zeta))^2}{\eta_{X_i}^2(\omega_i, \zeta)} - \Delta\omega \sum_{k=1}^{i-1} G(\omega_k) \right], & \omega_o \leq \omega_i \leq \omega_u \\ 0, & 0 \leq \omega_i < \omega_o \end{cases} \quad (10)$$

where  $U(\cdot)$  is the unit step function that is used to avoid negative solutions,  $\omega_u$  is an upper cut-off frequency,  $\omega_o = 0.36$  rad/s is the lowest frequency bound for  $\eta_{X_i}$  to exist [21], and  $\eta_{X_i}$  is the peak factor, which can be approximated with reference to a white noise input [21] as:

$$\eta_{X_i}(\omega_i, \zeta) = \sqrt{2 \ln \left\{ \frac{T_s}{\pi} \omega_i \left( -\ln \frac{1}{2} \right)^{-1} \left[ 1 - \exp \left( -\delta_{X_i}^{1.2} \sqrt{\pi \ln \left( \frac{T_s}{\pi} \omega_i \left( -\ln \frac{1}{2} \right)^{-1} \right)} \right) \right] \right\}} \quad (11)$$

where  $T_s$  is the duration of the stationary accelerogram, the mean zero crossing rate  $N_{X_i}$  is included in the equation, and the spread factor  $\delta_{X_i}$  is approximated as:

$$\delta_{X_i} = \sqrt{1 - \frac{1}{1 - \zeta^2} \left[ 1 - \frac{2}{\pi} \arctan \left( \frac{\zeta}{\sqrt{1 - \zeta^2}} \right) \right]^2} \quad (12)$$

Finally, regarding  $\varphi(t)$ , the time modulating function proposed by Jennings *et al.* [22] has been adopted:

$$\varphi(t) = \begin{cases} \left( \frac{t}{t_1} \right)^2, & t < t_1 \\ 1, & t_1 \leq t \leq t_2 \\ \exp \left[ -\frac{3}{t_f - t_2} (t - t_2) \right], & t > t_2 \end{cases} \quad (13)$$

where  $t_f$  is the total duration of the accelerogram. The time points  $t_1$  and  $t_2$  define the strong motion duration of the generated record and they can be obtained from the Husid function ( $H(t)$ ) of a real recorded accelerogram (Fig. 1) as  $H(t_1) = 5\%$  and  $H(t_2) = 95\%$  respectively (Fig. 2(a)). Alternatively, default values can be used instead [27]. In this frame,  $T_s$  is the duration of the strong motion, calculated as  $T_s = t_2 - t_1$ . Note that  $T_s$  signifies the constant amplitude region on the envelope function  $\varphi(t)$  (Fig. 2(b)).

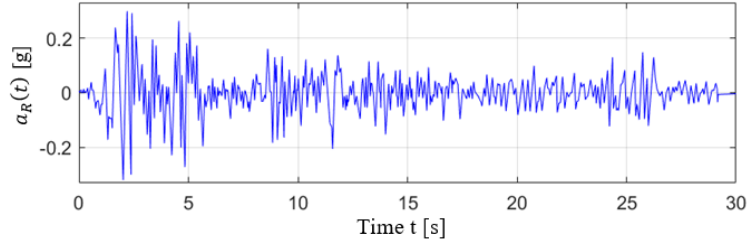


**Fig. 1.** A seed record accelerogram: El Centro earthquake (Imperial Valley, 1940, N-S component). The total duration of the accelerogram is  $t_f = 30$  s and the strong motion duration is  $T_s = t_2 - t_1 = 25.48\text{s} - 1.64\text{s} = 23.84$  s

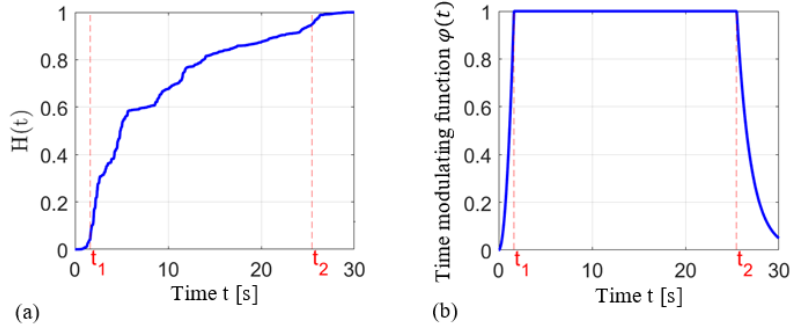


**Fig. 2.** (a) Husid plot of the El Centro recorded accelerogram of Fig.1, (b) the time modulating function of Eq. 13 obtained from the Husid plot of Fig. 2(a).

### 2.3 Record Correction

Artificial accelerogram generation methods usually require corrective iterations in the frequency domain in order to achieve good matching between the generated accelerogram's spectrum and the target spectrum. The most common corrective iteration method applied in the literature [e.g. in 15] utilizes the PSD function:

$$G(\omega_i)^{(k+1)} = G(\omega_i)^{(k)} \left[ \frac{S_a^*(\omega_i, \zeta)}{S_a^{(k)}(\omega_i, \zeta)} \right]^2 \quad (14)$$



where  $S_a^{(k)}(\omega_i, \zeta)$  is the generated accelerograms' mean response spectrum determined at the  $k^{\text{th}}$  iteration. In the proposed model, however, in order to control the variability of the analysis, the corrective iterations are applied in each of the generated accelerograms spectrum  $S_a^j(\omega_i, \zeta)$  individually, with their respective target spectrum  $S_a^{*,j}(\omega_i, \zeta)$ . Moreover, it is essential that the spectrum matching should be perfect, as it was observed that insufficient matching would result in significant differences between the target and the analysis variability. Corrective iterations with the aforementioned requirements and the use of the PSD function were proved to not be sufficient enough to control the variability of the analysis. Therefore, as corrective iterations are conducted in the frequency domain, the Fourier Transform (FT) was employed. For each frequency, the accelerogram's Fourier Transform (FT) is modified by the quotient of  $S_a^{*,j}(\omega_i, \zeta)$  and  $S_a^j(\omega_i, \zeta)$ , as follows [23]:

$$FT_{a_g(t)}^{(k+1)}(\omega_i) = FT_{a_g(t)}^{(k)}(\omega_i) \left[ \frac{S_a^{*,j}(\omega_i, \zeta)}{S_a^j(\omega_i, \zeta)} \right] \quad (15)$$

where  $FT_{a_g(t)}^{(k)}(\omega_i)$  is the Fourier Transform of the generated accelerogram at the  $k^{\text{th}}$  iteration. Then, by applying the inverse Fourier Transform, a new time-history  $a_g^{(k+1)}(t)$  is determined, along with its response spectrum  $S_a^{j,(k+1)}(\omega_i, \zeta)$ . The iteration scheme provided by Eq. 15 modifies the spectral amplitude characteristics of the generated accelerogram. Fig. 3 shows an example of the difference in the Fourier amplitude of an accelerogram simulated with the seed record approach before the corrective iterations (i.e. as generated) and after.

Finally, each of the generated accelerograms requires baseline correction in order to yield realistic velocity and displacement time-histories. In this study, a simple cubic polynomial curve is used for baseline correcting the generated ground motions.

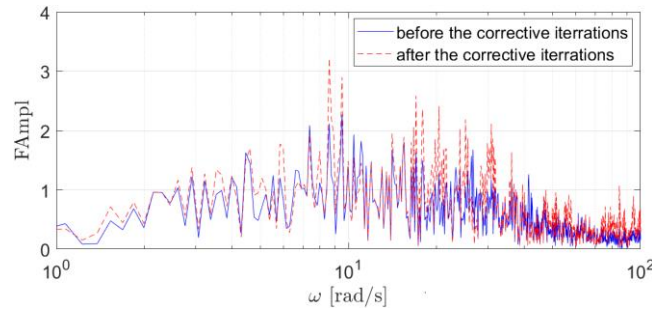


**Fig. 3.** Comparison of the Fourier amplitude of a simulated accelerogram before and after the corrective iterations for spectrum compatibility.

### 3 Seismic Performance Assessment to Artificial Ground Motions Records

#### 3.1 Case Study Considered

The aim of this paper is to present a practical application of the methodology proposed in [12,19–21], through the NRHA of a benchmark multi-degree-of-freedom (MDOF) structure. Two cases are considered where: i) the generated suite of ground motions matches only a mean target spectrum, and ii) the generated suite of ground motions matches both a mean target spectrum and target variability. The seismic hazard is quantified with a GMM which provides the median target spectrum and the logarithmic standard deviations. The GMM employed in this study is the BSSA 14 [17]. The seismic scenario considered is of moment magnitude  $M_w = 6.5$ , Joyner-Boore distance  $R_{JB} = 10$  km, and  $\epsilon = 1$ . The shear wave velocity averaged over the top 30 m  $V_{S30}$  is set equal to 360 m/s, the damping ratio is  $\zeta = 5\%$ , the fault type is normal, and the basin depth is set unknown. The case study frame is an eight-storey steel moment-resisting frame with the properties shown in Fig. 4(a).

The frame and the analysis are implemented with OpenSees v3.5.0. The gravity loads ( $q=40$  kN/m) and the respective masses are concentrated at the nodes. The members are modeled as force-based, beam-column fiber elements with four integration sections for the NRHA and the material is a uniaxial bilinear steel material object with kinematic hardening. No geometric non-linearities are incorporated. After performing modal analysis with elastic beam-column elements, the fundamental period was found equal to  $T_1 = 3.59$  s with mass modal participation of the first mode equal to 82% of the total mass. Thus, the frame is dominated by the first mode (Fig. 4(b)), however the second mode also contributes to the response with  $T_2 = 1.17$  s and mass modal participation equal to 10% ( $82\% + 10\% = 92\% > 90\%$  as defined by the Eurocode 8 [4]). Rayleigh damping is used with Rayleigh damping coefficients  $\alpha_0 = 0.13$  and  $\alpha_1 = 0.014$ .

For each case, seven accelerograms are generated in order to conduct NRHAs on the eight-storey steel moment-resisting frame. The investigated response parameters are the maximum interstorey drift ratios (MIDR) in terms of median and dispersion (16<sup>th</sup> and 85<sup>th</sup> percentile values). The chosen number of generated accelerograms is consistent with seismic code provisions, which require at least seven NRHAs in order to characterize statistically the seismic input and structural seismic response.

The seed record method [15] is applied to generate the artificial non-stationary accelerograms, following Eqs. 7–13. The frequency range is  $\omega_0=1$  rad/s,  $\omega_u=100$  rad/s,  $N = 1000$ , and  $\Delta\omega = 0.10$  rad/s. In this example, the seed record selected is the 24/2/1981 Gulf of Corinth earthquake (Corinth Greece, 24/2/1981, Corinth, T component, Fig. 5) from the Pacific Earthquake Engineering Centre (PEER) [24], as it belongs to a compatible scenario of  $M_w = 6.6$ ,  $R_{JB} = 10.27$  km,  $V_{S30} = 361.40$  m/s, and normal oblique fault type. The total duration of the accelerogram is  $t_f = 40.93$  s and the strong motion duration is  $T_s = t_2 - t_1 = 17.72$  s – 3.78 s = 13.94 s. Finally, corrective iterations are performed following Eq. 15 and baseline correction is applied.

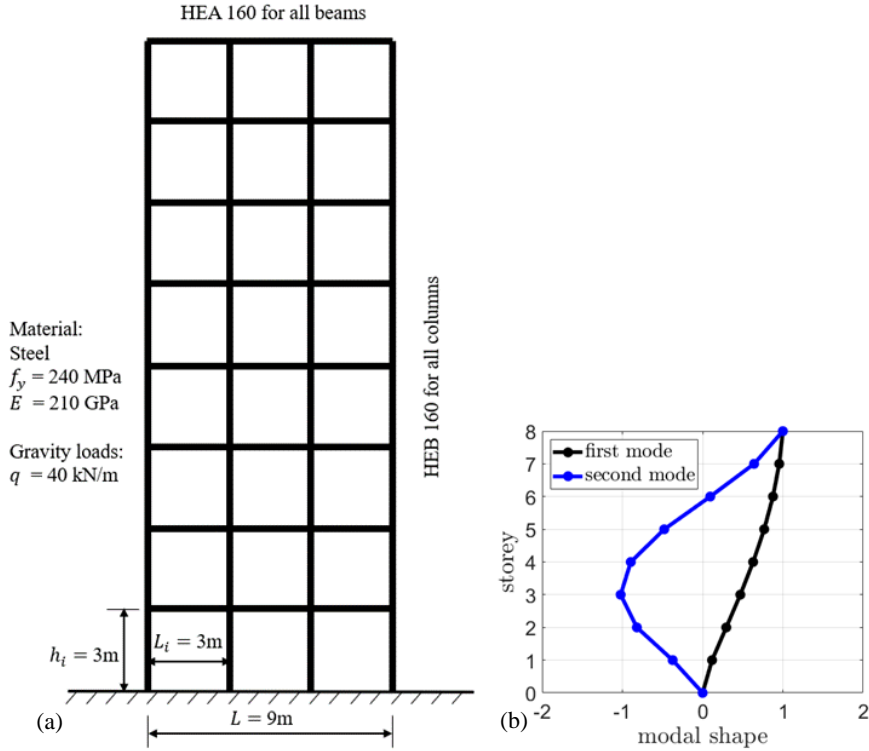


**Fig. 4.** (a) The benchmark structure: the eight-story steel frame of the second numerical application, used for the NRHAs, (b) The first and second mode of the benchmark eight-storey steel moment-resisting frame.

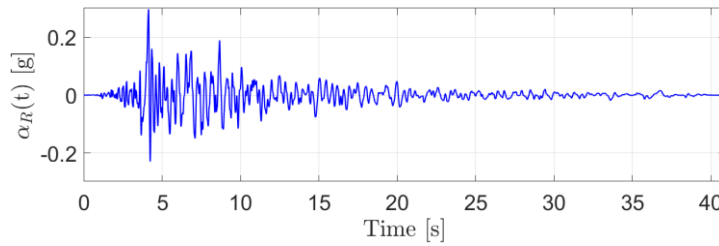


**Fig. 5.** The seed record accelerogram of the second numerical application: Corinth Greece, 24/2/1981, Corinth, T component.

### 3.2 Case 1: NRHAs using a generated suite of ground motions that matches only a mean target spectrum

A suite of seven fully non-stationary accelerograms is generated using Eqs. 1–2 for the target median spectrum  $S_a^*(T_i, \zeta)$  obtained from the GMM and the variability is set equal to  $\beta^*(T_i, \zeta) = 0$ . The median response spectrum of the produced accelerograms is shown

in Fig. 6 along with the target  $S_a^*(T_i, \zeta)$ . The comparisons are made in median values, considering the mathematical property that the median of data that follow a lognormal distribution is approximately equal to the mean of the logarithms.

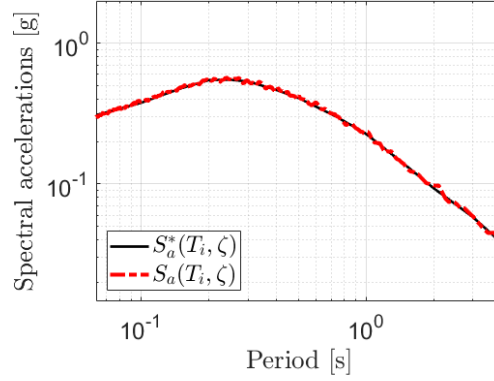


**Fig. 6.** The produced target response spectra  $S_a^{*j}(T_i, \zeta)$  of the second numerical application following Eqs. 1–2, for the generation of 7 accelerograms.

The produced accelerograms are used for the NRHAs of the benchmark eight-storey steel moment-resisting frame and the median and dispersion values of the MIDRs are obtained and plotted in Fig. 7.

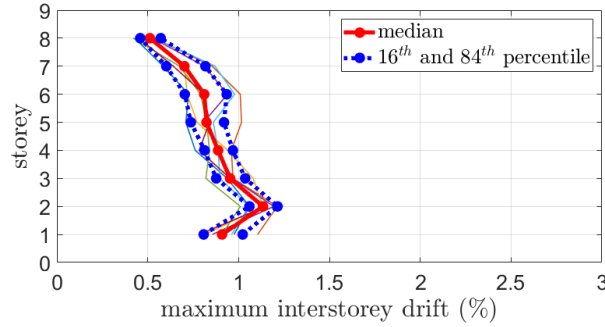


**Fig. 7.** The MIDRs of the eight-storey steel moment-resisting frame using a generated suite of ground motions that matches only the mean target spectrum.

### 3.3 Case 2: NRHAs using a generated suite of ground motions that matches both a target mean spectrum and variability

A suite of seven fully non-stationary accelerograms is generated, and the target mean  $S_a^*(T_i, \zeta)$  and variability  $\beta^*(T_i, \zeta) = \sigma_{\ln(S_a)}^*(T_i, \zeta)$  of the suite are obtained from the GMM. The produced spectra  $S_a^{*j}(T_i, \zeta)$  are obtained following Eqs. 1–2 and they are shown in Fig. 8 along with the target  $S_a^*(T_i, \zeta)$  that is obtained from the aforementioned GMM. Note that the assumed perfect direct correlation results in equally distanced values of a produced spectrum  $S_a^{*j}(T_i, \zeta)$  from the target  $S_a^*(T_i, \zeta)$ .

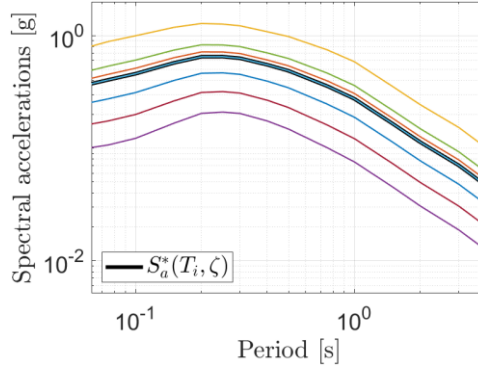


**Fig. 8.** The produced target response spectra  $S_a^{*j}(T_i, \zeta)$  of the second numerical application following Eqs. 1–2, for the generation of seven accelerograms.

The comparison between the target spectrum  $S_a^{*j}(T_i, \zeta)$  and the median response spectrum  $S_a(T_i, \zeta)$  of the generated accelerograms is shown in Fig. 9(a). Furthermore, Fig. 9(b) shows the matching of the analysis variability  $\beta(T_i, \zeta) = \sigma_{\ln(S_a)}(T_i, \zeta)$  achieved with the proposed model (standard deviation of the natural logarithms) to the target  $\beta^{*j}(T_i, \zeta) = \sigma_{\ln(S_a^{*j})}^{*j}(T_i, \zeta)$ . As it can be observed, for both the spectral mean and variance, the simulated values are remarkably close to the set targets, thus proving the efficiency of the proposed algorithm.

The produced accelerograms are then used for the NRHAs of the case study frame and the median and 16<sup>th</sup> and 85<sup>th</sup> percentile values of the MIDRs are obtained and plotted in Fig. 11.

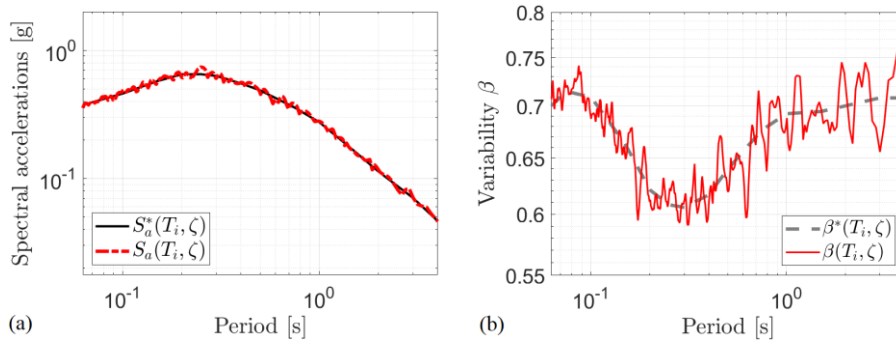


**Fig. 9.** (a) Comparison of the generated accelerograms' median response spectrum  $S_a(T_i, \zeta)$  matching to the target median spectrum  $S_a^{*j}(T_i, \zeta)$  of the second numerical application. (b) comparison of the analysis variability  $\beta(T_i, \zeta) = \sigma_{\ln(S_a)}(T_i, \zeta)$  with the target  $\beta^{*j}(T_i, \zeta) = \sigma_{\ln(S_a^{*j})}^{*j}(T_i, \zeta)$

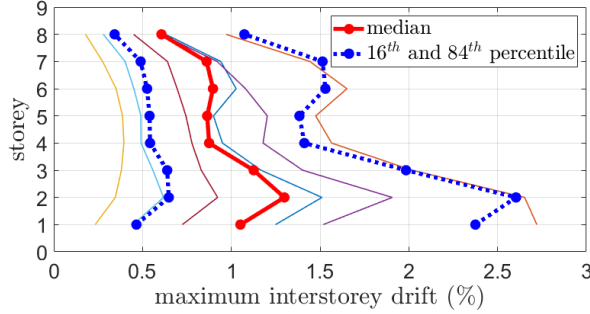


**Fig. 11.** The MIDRs of the eight-storey steel moment-resisting frame estimated through NRHAs using a generated suite of ground motions that matches both a target mean spectrum and variability.

### 3.4 Result Comparison

Table 1 summarizes the MIDR estimates of the two cases in terms of median and 16<sup>th</sup> and 85<sup>th</sup> percentile values. It is observed that the median values are close for both cases, whereas the dispersion values differ significantly. Specifically, in the case where the variability of the target spectrum is incorporated in the generation of the ground motion suite, the dispersion of the MIDRs is larger, as expected. These results are compatible with the similar observations of Jayaram et al. [2] for their record selection algorithm, which state that when the response spectrum variability is considered in the ground motion selection procedure, the median structural response is not significantly affected, whereas the dispersion in the response tends to increase. These results prove that the proposed methodology produces realistic results for NRHAs and complete the testing of the efficiency of the proposed methodology for practical applications.

**Table 1.** MIDR estimates of the case study frame. The Case 1 results correspond to the suite of ground motions who match only the target spectral mean, whereas the Case 2 results correspond to the suite of ground motions who match both the target spectral mean and variability.

Storey	Median MIDR %			Dispersion of MIDR %		
	Case 1	Case 2	error %	Case 1	Case 2	error %
1	0.91	1.05	15.7	11.79	81.49	590.95
2	1.13	1.30	14.5	6.82	69.54	919.09
3	0.95	1.13	18.0	8.36	56.68	577.70
4	0.89	0.87	-1.4	8.79	47.83	444.28
5	0.82	0.86	4.9	11.04	47.10	326.41
6	0.81	0.90	10.6	14.18	53.42	276.74
7	0.70	0.86	22.6	15.26	56.48	270.06
8	0.51	0.61	18.5	10.99	57.10	419.79

## 4 Conclusions and Discussion

The efficiency of a novel stochastic methodology for the generation of suites of fully non-stationary artificial accelerograms that are compatible both with a target mean spectrum and a target variability has been tested through the NRHAs of a benchmark frame. Hazard consistency has been defined by obtaining the target spectral mean and variability from a GMM and the ground motions have been generated using widely known spectral representation techniques. This paper assumes that the correlations between spectral acceleration values at multiple periods are equal to 1. It should be noted that Eq. 1 in [12] is extended to a more general case, where the CMS can also be employed in the analyses and the correlations will also be possible to be included in the spectra simulation process.

The methodology has been tested in order to ensure that the produced suites of ground motions provide realistic NRHA estimates. The results of the NRHAs of an eight-storey steel moment-resisting frame which was subjected to two cases of ground motion suites were compared. One suite of ground motions matched only a mean target spectrum, whereas the other suite of ground motions matched both a mean target spectrum and target variability. The results showed that in the latter case, the median structural response is not significantly affected, whereas the dispersion in the response tends to increase.

A point worth noting is that the present work simplifies the methodology proposed in [12] and uses accelerograms with a fixed power spectrum and modulating function values. This results in suites of artificial accelerograms that have very similar time-frequency features, however, this simplification has been adopted in order to focus on the influence of the target spectrum variability on the structural estimates without having additional uncertainties added.

In conclusion, the obtained results of this study were compatible with similar observations from relative ground motion selection algorithms in the literature. Thus, the proposed methodology produces realistic results for NRHAs and is efficient for practical applications.

## 5 Acknowledgements

The authors gratefully acknowledge the support by the Hellenic Foundation for Research and Innovation (Grant No. 1261).

## References

1. Dávalos, H., Miranda, E.: Evaluation of bias on the probability of collapse from amplitude scaling using spectral-shape-matched records. *Earthquake Engineering & Structural Dynamics* 48(8), 970–986 (2019). <https://doi.org/10.1002/eqe.3172>.
2. Jayaram, N., Lin, T., Baker, J.: A Computationally efficient ground-motion selection algorithm for matching a target response spectrum mean and variance. *Earthquake Spectra* 27(3), 797–815 (2011). <https://doi.org/10.1193/1.3608002>.

3. Georgioudakis, M., Fragiadakis, M.: Selection and Scaling of Ground Motions Using Multicriteria Optimization. *American Society of Civil Engineers (ASCE)* 146(11), 04020241 (2020). [https://doi.org/10.1061/\(ASCE\)ST.1943-541X.0002811](https://doi.org/10.1061/(ASCE)ST.1943-541X.0002811).
4. Comité Européen de Normalisation (CEN): EN 1998-1-1 (Eurocode 8): Design of structures for earthquake resistance, part 1: general rules, seismic actions and rules for buildings, Brussel, (2004).
5. Song, C., Kawai, R.: Monte Carlo and variance reduction methods for structural reliability analysis: A comprehensive review. *Probabilistic Engineering Mechanics* 73, 103479 (2023). <https://doi.org/10.1016/j.probengmech.2023.103479>.
6. Mitseas, I.P., Beer, M.: Fragility analysis of nonproportionally damped inelastic MDOF structural systems exposed to stochastic seismic excitation. *Computers and Structures* 226, 106129 (2020). <https://doi.org/10.1016/j.compstruc.2019.106129>.
7. Mitseas, I.P., Beer, M.: First-excursion stochastic incremental dynamics methodology for hysteretic structural systems subject to seismic excitation. *Computers and Structures* 242 (2021). <https://doi.org/10.1016/j.compstruc.2020.106359>.
8. Psycharis, I.N., Fragiadakis, M., Stefanou, I.: Seismic reliability assessment of classical columns subjected to near-fault ground motions. *Earthquake Engineering & Structural Dynamics* 42(14), 2061–2079 (2013).
9. Shinozuka, M., Deodatis, G.: Simulation of Stochastic Processes by Spectral Representation. *Applied Mechanics Reviews* 44(4), 191–204, (1991). <https://doi.org/10.1115/1.3119501>.
10. Vanmarcke, E.H., Gasparini, D.A.: Simulated earthquake ground motions. In: *Proceedings of the 4th international conference on structural mechanics in reactor technology, K1/9*, San Francisco, CA, USA, (1977).
11. Spanos, P., Vargas Loli L.M.: A statistical approach to generation of design spectrum compatible earthquake time histories. *International Journal of Soil Dynamics and Earthquake Engineering* 4(1), 2–8 (1985). [https://doi.org/10.1016/0261-7277\(85\)90029-4](https://doi.org/10.1016/0261-7277(85)90029-4).
12. Yanni, H., Fragiadakis, M., Mitseas, I.P.: Probabilistic method for the generation of hazard-consistent suites of fully non-stationary seismic records. *Earthquake Engineering & Structural Dynamics* 53(10), 3140–3164 (2024). <https://doi.org/10.1002/eqe.4153>.
13. Preumont A.: The generation of non-separable artificial earthquake accelerograms for the design of nuclear power plants. *Nuclear Engineering and Design* 88(1), 59–67 (1985). [https://doi.org/10.1016/0029-5493\(85\)90045-7](https://doi.org/10.1016/0029-5493(85)90045-7).
14. Yanni, H., Fragiadakis, M., Mitseas, I.P.: Stochastic generation of artificial accelerograms using the continuous wavelet transform method. In: *Proceedings of the 9th International Conference on Computational Methods in Structural Dynamics and Earthquake Engineering (COMPDYN 2023)*, June 12-14, Athens, Greece (2023).
15. Cacciola, P.: A stochastic approach for generating spectrum compatible fully nonstationary earthquakes. *Computers & Structures* 88(15–16), 889–901 (2010).
16. Baker, J.: Conditional Mean Spectrum: Tool for Ground-Motion Selection. *Journal of Structural Engineering* 137(3), 322–331 (2011). [https://doi.org/10.1061/\(ASCE\)ST.1943-541X.0000215](https://doi.org/10.1061/(ASCE)ST.1943-541X.0000215).
17. Boore, D.M., Stewart, J.P., Seyhan, E., Atkinson, G.M.: NGA-West2 Equations for Predicting PGA, PGV, and 5% Damped PSA for Shallow Crustal Earthquakes. *Earthquake Spectra* 30(3), 1057–1085 (2014). <https://doi.org/10.1193/070113EQS184M>.
18. National Institute of Standards and Technology (NIST): Selecting and scaling earthquake ground motions for performing response history analyses. Rep. No. NIST GCR 11-917-15. East Lansing, MI: NEHRP Consultants Joint Venture, (2011).



19. Yanni, H., Fragiadakis, M., Mitseas, I.P.: A novel method for the stochastic generation of artificial accelerograms. In: Proceedings of the 5th Panhellenic Conference on Earthquake Engineering and Engineering Seismology. Hellenic Association for Earthquake Engineering. October 20-22, Athens, Greece (2022).
20. Yanni, H., Fragiadakis, M., Mitseas, I.P.: A novel stochastic methodology for the generation of artificial seismic accelerograms. In: Proceedings of the XII International Conference on Structural Dynamics (EURODYN 2023), European Association for Structural Dynamics. June 02-05, Delft, The Netherlands (2023).
21. Cacciola, P., Colajanni, P., Muscolino, G.: Combination of Modal Responses Consistent with Seismic Input Representation. *Journal of Structural Engineering* 130(1), 47–55 (2004). [https://doi.org/10.1061/\(ASCE\)0733-9445\(2004\)130:1\(47\)](https://doi.org/10.1061/(ASCE)0733-9445(2004)130:1(47)).
22. Jennings, P.C., Housner, G.W., Tsai, C.: Simulated earthquake motions for design purpose In: Proceedings of the 4th World Conference Earth. Eng., Santiago, Vol. A-1, pp. 145–60; (1969).
23. Ferreira, F., Moutinho, C., Cunha, Á., Caetano, E.: An artificial accelerogram generator code written in Matlab. *Engineering Reports* 2(3), 92020). <https://doi.org/10.1002/eng2.12129>.
24. PEER (Pacific Earthquake Engineering Research Center). Shallow crustal earthquakes in active tectonic regimes. <https://ngawest2.berkeley.edu/site>.
25. MathWorks. MATLAB version 2021a [Computer Program]. <https://www.mathworks.com/products/matlab.html>.